

**$U_A(1)$ SYMMETRY RESTORATION
FROM AN IN-MEDIUM η' MASS REDUCTION
IN $\sqrt{s_{NN}} = 200$ GEV Au+Au COLLISIONS ***

T. CSÖRGÖ

*Dept. Physics, Harvard University,
17 Oxford Street, Cambridge, MA 02138, USA,
and*

*MTA KFKI RMKI,
H-1525 Budapest 114, P.O.Box 49, Hungary
E-mail: csorgo@rmki.kfki.hu*

R. VÉRTESI AND J. SZIKLAI

*MTA KFKI RMKI,
H-1525 Budapest 114, P.O.Box 49, Hungary
E-mails: vertesi@rmki.kfki.hu, sziklai@rmki.kfki.hu*

A reduction of the mass of the η' (958) meson may signal restoration of the $U_A(1)$ symmetry in a hot and dense hadronic matter, corresponding to the return of the 9th, "prodigal" Goldstone boson. We report on an analysis of a combined PHENIX and STAR data set on the intercept parameter of the two-pion Bose-Einstein correlation functions, as measured in $\sqrt{s_{NN}} = 200$ GeV Au+Au collisions at RHIC. To describe this combined PHENIX and STAR dataset, an in-medium η' mass reduction of at least 200 MeV is needed, at the 99.9 % confidence level in a broad model class of resonance abundances.

1. Introduction

Although the quark model exhibits a $U(3)$ chiral symmetry in the limit of massless up, down and strange quarks, and in principle 9 massless Goldstone modes are expected to appear when this symmetry is broken, only 8 light pseudoscalar mesons are observed experimentally. This puzzling mystery is resolved by the Adler-Bell-Jackiw $U_A(1)$ anomaly: instantons tunneling between topologically different QCD vacuum states explicitly

*This work is supported by the Hungarian OTKA grant NK73143 and by HAESF, the Hungarian-American Enterprise Scholarship Fund.

break the $U_A(1)$ part of the $U(3)$ symmetry. Thus the 9th Goldstone boson is expected to be massive, and is associated with the η' meson, which has a mass of 958 MeV, approximately twice that of the other pseudoscalar mesons.

In high energy heavy ion collisions at RHIC, a hot and dense medium is created. Recent measurements of the direct photon spectrum in $\sqrt{s_{NN}} = 200$ GeV Au+Au collisions indicate ¹, that the initial temperature in these reactions is at least 300 MeV, while hadrons as we know them may not exist above the Hagedorn temperature of $T_H \approx 170$ MeV ². Thus the matter created in heavy ion collisions at RHIC is hot enough to be a quark-gluon plasma ¹. Detailed analysis of the properties of this matter indicate that it flows like a perfect fluid ³, and scaling properties of the elliptic flow indicate scaling with the number of constituent quarks ⁴, hence this matter is sometimes referred to as a strongly interacting Quark-Gluon Plasma (sQGP) ⁵, or, in more direct terms, a perfect fluid of quarks ³.

After this perfect fluid of quarks rehadronizes, a hot and dense hadronic matter may be created, where the $U_A(1)$ symmetry of the strong interactions may temporarily be restored ^{6,7,8}. Recent lattice QCD calculations indicate that such chirally symmetric but hadronic matter may exist below the critical temperature for quark deconfinement ⁹. In such a medium, the mass of the $\eta'(958)$ mesons may be reduced to its quark model value of about 500 MeV, corresponding to the return of the “prodigal” 9th Goldstone boson ⁷. Here we report on an indirect observation of such an in-medium η' mass modification based on a detailed analysis of PHENIX and STAR charged pion Bose-Einstein correlation (BEC) data ^{10,11}.

The abundance of the η' mesons with reduced mass may be increased at low p_T , by more than a factor of 10. One should emphasize that the η' (and η) mesons almost always decay after the surrounding hadronic matter has frozen out, due to their small annihilation and scattering cross sections, and their decay times that are much longer than the characteristic 5-10 fm/c decoupling times of the fireball created in high energy heavy ion collisions. Therefore one cannot expect a direct observation of the mass shift of the η' (or η) mesons: all detection possibilities of their in-medium mass modification have to rely on their enhanced production.

An enhancement of low transverse momentum η' mesons contributes to an enhanced production of soft charged pions mainly through the $\eta' \rightarrow \eta + \pi^+ + \pi^- \rightarrow (\pi^+ + \pi^0 + \pi^-) + \pi^+ + \pi^-$ decay chain and also through other, less prominent channels. As the η' decays far away from the fireball, the enhanced production of pions in the corresponding halo

region will reduce the strength of the Bose-Einstein correlation between soft charged pions. The transverse mass ($m_T = \sqrt{m^2 + p_T^2}$) dependence of the extrapolated intercept parameter λ_* of the charged pion Bose-Einstein correlations was shown to be an observable that is sensitive to such an enhanced η' multiplicity, as pointed out first in Ref. ¹⁴ and discussed in Ref. ¹⁵. The predicted decrease of $\lambda_*(m_T)$ data at low transverse mass has been observed both by PHENIX ¹⁰ and STAR ^{11,12} at RHIC.

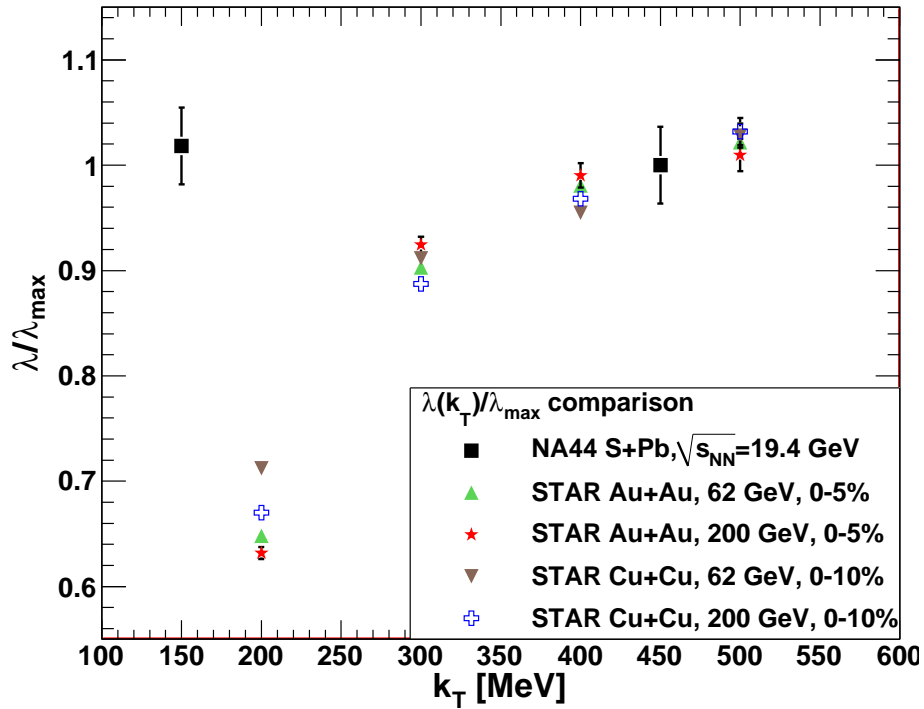


Figure 1. The energy and system size dependence of the relative intercept parameter in the NA44 S+Pb and STAR Cu+Cu and Au+Au datasets.

Figure 1 indicates that a “hole” at low transverse mass, in the region characteristic to the $\eta' \rightarrow \eta + \pi^+ + \pi^- \rightarrow \eta' \rightarrow (\pi^+ \pi^0 \pi^-) + \pi^+ + \pi^-$ decay chain is not present in the S+Pb data set at CERN SPS at $\sqrt{s_{NN}} = 19.4$ GeV energy ¹³, however, it is present and becomes slightly deeper as the system size and the colliding energy is increased from Cu+Cu to Au+Au and from $\sqrt{s_{NN}} = 62.4$ GeV to 200 GeV ¹².

2. Modeling and analysis method

Our main analysis tool was a Monte-Carlo simulation of the transverse mass dependence of the long lived resonance multiplicities including the possibility of an enhanced η' production at low transverse momentum, due to a partial in-medium $U_A(1)$ restoration and a related η' mass modification. This model and the related reduction of the effective intercept parameter of the two-pion Bose-Einstein correlation function was proposed first in ref. ¹⁴ and detailed recently in Refs. ^{16,17,18}.

In thermal models, the production cross sections of the light mesons are exponentially suppressed by the mass. Hence one expects about two orders of magnitude less η' mesons from the freeze-out than pions. This suppression, however, may be moderated as a consequence of a possible η' mass reduction, and the η' mesons may show up in an enhanced number. The number of in-medium η' mesons is calculated with an improved Hagedorn formula yielding the following η' enhancement factor:

$$f_{\eta'} = \left(\frac{m_{\eta'}^*}{m_{\eta'}} \right)^\alpha e^{-\frac{m_{\eta'} - m_{\eta'}^*}{T_{cond}}}. \quad (1)$$

This formula includes a prefactor with an expansion dynamics dependent exponent $\alpha \approx 1 - d/2$ for an expansion in d effective dimensions ¹⁹. As a default value, $\alpha = 0$ was taken ¹⁴ and, for the systematic investigations, this parameter was varied between $-0.5 \leq \alpha \leq 0.5$. Other model parameters and their investigated ranges are described as follows: T_{cond} in the above formula corresponds to the temperature of the medium when the in-medium modified η' mesons are formed; its default value was taken to be $T_{cond} = 177$ MeV ¹⁴ and varied systematically between 140 and 220 MeV. Resonances with different masses were simulated with a mass dependent slope parameter $T_{eff} = T_{FO} + m\langle u_T \rangle^2$, where the default values of $T_{FO} = 177$ MeV and $\langle u_T \rangle = 0.48$ ²⁰ were utilized and systematically varied in the range of $100 \text{ MeV} \leq T_{FO} \leq 177 \text{ MeV}$ and $0.40 \leq \langle u_T \rangle \leq 0.60$.

Once produced, the η' is expected to be decoupled from other hadronic matter, since its annihilation and scattering cross sections are very small ⁷. If the η' mass is reduced in the medium, the observed η' spectrum will consist of two components. If the p_T of the η' is large enough, it can get on-shell and escape. This will produce a thermal component of the spectrum. Energy conservation at mid-rapidity implies $m_{\eta'}^{*2} + p_{T,\eta'}^{*2} = m_{\eta'}^2 + p_{T,\eta'}^2$. (In the latter equation the quantities marked with an asterisk denote the properties of the in-medium η' , while the ones without an asterisk refer to the free η' .) On the other hand, η' -s with $p_{T,\eta'}^* \leq \sqrt{m_{\eta'}^{*2} - m_{\eta'}^2}$ will not

be able to leave the hot and dense region through thermal fluctuation since they cannot compensate for the missing mass^{7,8}, and thus will be trapped in the hot and dense region until it disappears. As the energy density of the medium is dissolved, the effect of QCD instantons increases and the trapped η' mesons regain their free mass and appear at low p_T .

In our recent works of Refs.^{16,17,18}, we improved on earlier simulations of Ref.¹⁴, that considered the trapped η' mesons to leave the dissolving medium with a negligible p_T . That earlier approach resulted in a steep hole in the extrapolated intercept parameter $\lambda_*(m_T)$ at a characteristic transverse mass of $m_T \leq 250$ MeV^{14,15,21}. In that simplified scenario the only free parameter was the in-medium η' mass, determining the depth of the observed hole. In a recent analysis, summarized here, the η' -s from the decaying condensate were given a random transverse momentum, following Maxwell-Boltzmann statistics with an inverse slope parameter B^{-1} , which was necessary to obtain a quality description of the width and the slope of the $\lambda_*(m_T)$ data of PHENIX and STAR in the $m_T \approx 300$ MeV region. Physically, B^{-1} is limited by T_{FO} , so the trapped η' -s may gain only moderate transverse momenta. Hence, the enhancement mostly appears at low p_T ^{6,7,8} just as in the first simulations. However, now the slope of “hole” of the $\lambda_*(m_T)$ curve is determined by B^{-1} , and, for certain values of the model parameters, the data can be reproduced quantitatively. (The λ_* values, actually used in the presented analysis, and their total errors are discussed in details in Ref.¹⁸. Here λ_*^{\max} is the $\lambda_*(m_T)$ value taken at $m_T = 0.7$ GeV, with the exception of the STAR data, where the data point at the highest $m_T = 0.55$ GeV is considered. Note that the m_T dependency of the $\lambda_*(m_T)$ measurements in the 0.5-0.7 GeV region is very weak.)

We have investigated a broad class of models of resonance production, including two different models that produce resonances without assuming local thermalization: FRITIOF²² and UrQMD²³. Resonance decays, including decay chains, were simulated with JETSET 7.4²⁴.

The FRITIOF²² Monte Carlo model, based on superposition of nucleon-nucleon collisions and the Lund string fragmentation model, cannot describe the behavior seen in $\lambda_*(m_T)/\lambda_*^{\max}$ even when an arbitrary η' mass modification is considered. On the other hand, hadronic cascade based UrQMD²³, as well as the quark coalescence model ALCOR²⁵ and the thermal resonance production models of refs.^{26,28,27}, provide a successful fit in a certain range of the in-medium η' masses. The main difference between the thermal models that we utilized was in those resonance multiplicities that are not yet measured well: ref.²⁶ predicts a factor of 1.6 more

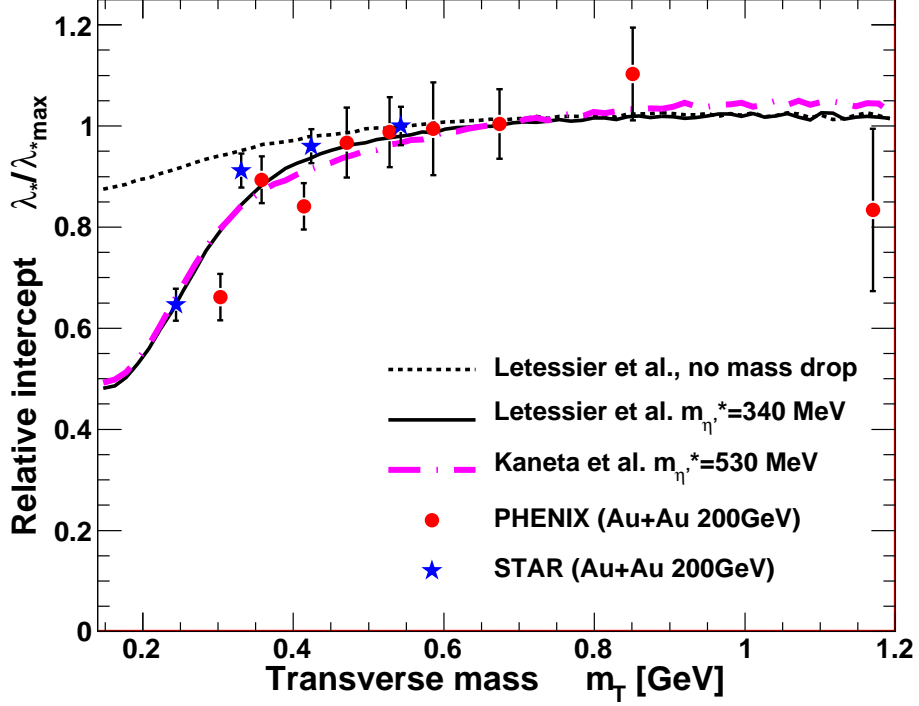


Figure 2. The transverse mass dependence of the relative intercept parameter in the PHENIX and STAR dataset is reproduced with an in-medium mass modification of the η' mesons using two different resonance models as input. The same resonance models, but without in-medium mass modification, cannot explain these datasets.

η -s and a factor of 3 more η' -s than the models of ref. ^{27,28}. The relevant resonance fractions of these models are detailed in Table V of ref. ¹⁸.

The dotted line in Fig. 2 indicates a scenario without an in-medium η' mass reduction, while the dot-dashed and solid lines show the enhancement required to describe the dip in the low m_T region of λ_* corresponding to the resonance multiplicities of Refs. ^{26,27}, respectively.

Based on extensive Monte-Carlo simulations, χ^2 of the fits to the data of Fig. 2 was computed as a function of $m_{\eta'}^*$ and B^{-1} for each resonance model and each fixed value of model parameters of α , T_{cond} , T_{FO} and $\langle u_T \rangle$. The best values for the in-medium mass of η' mesons are in, or slightly below, the range $\sqrt{\frac{1}{3}(2m_K^2 + m_\pi^2)} \leq m_{\eta'}^* \leq \sqrt{2m_K^2 - m_\pi^2}$ predicted in ref. ⁷, while all are above the lower limit of $m_{\eta'}^* \geq \sqrt{3}m_\pi$ given by

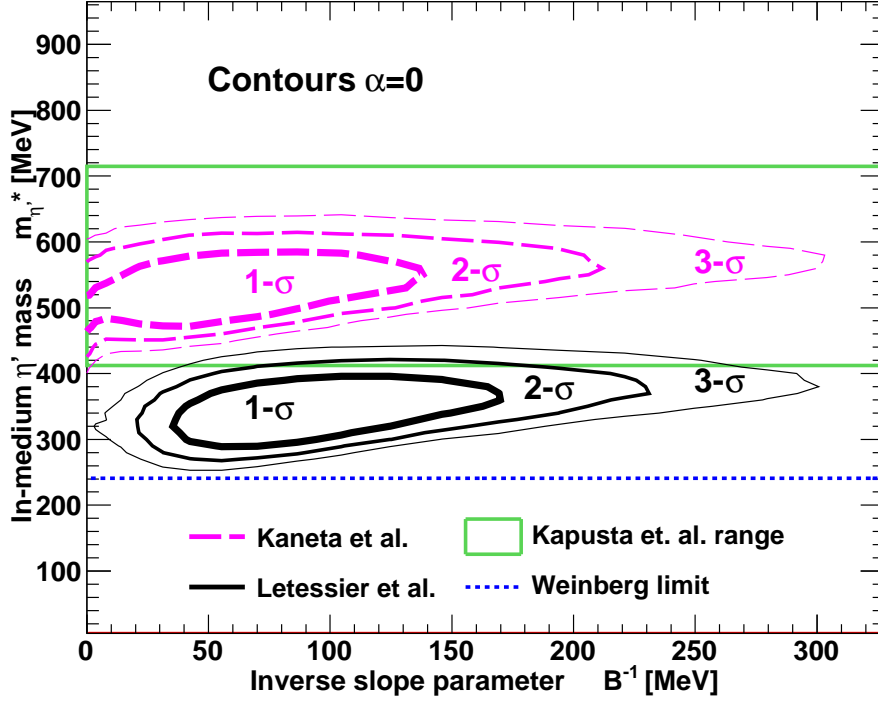


Figure 3. Standard deviation contours on the $(B^{-1}, m_{\eta'}^*)$ plane, obtained from $\lambda_*(m_T)/\lambda_*^{max}$ of Monte Carlo simulations based on particle multiplicities using two different models for hadronic resonances. The region between the horizontal solid lines indicates the theoretical range predicted by quark model considerations, while the dotted horizontal line stands for Weinberg's lower limit.

ref. ²⁹. The $\lambda_*(m_T)/\lambda_*^{max}$ simulations for the best fits of two characteristic models are compared to the no-mass-drop scenario on Fig. 2, while the 1, 2 and 3- σ parameter boundaries are indicated in Fig. 3. Those models that describe both PHENIX and STAR $\lambda_*(m_T)/\lambda_*^{max}$ data in a statistically acceptable manner with the assumption of a sufficiently large in-medium η' mass reduction are all used for the estimation of systematics. The key parameters of the best fits are listed in Table 1.

3. Results

We have used different input models and setups to map the parameter space for a twofold goal: to determine, at least how big η' in-medium mass reduction is needed to be able to describe these datasets, and also to

determine, what are the best values of the in-medium mass modification of the η' mesons. Utilizing our indirect method, we have also reconstructed the transverse mass dependent spectrum of these η' mesons.

3.1. Lower limit on the in-medium η' mass reduction

We excluded certain regions where a statistically acceptable fit to the data is not achievable, thus we can give a lower limit on the η' mass modification. At the 99.9 % confidence level, corresponding to a more than 5- σ effect, at least 200 MeV in-medium decrease of the mass of the η' (958) meson was needed to describe both STAR 0-5 % central and PHENIX 0-30% central Au+Au data on $\lambda_*(m_T)/\lambda_*^{max}$ in $\sqrt{s_{NN}} = 200$ GeV Au+Au collisions at RHIC, in the considered model class.

3.2. Best value of the in-medium η' mass reduction

We have determined the best values and errors of the fitted $m_{\eta'}^*$ and B^{-1} parameters. The best simultaneous description of PHENIX¹⁰ and STAR¹¹ relative intercept parameter data is achieved with an η' mass that is dramatically reduced in the medium created in central Au+Au collisions at RHIC from its vacuum value of 958 MeV to $340_{-60}^{+50}{}_{-140}^{+280} \pm 45$ MeV. The first error here is the statistical one determined by the 1- σ boundaries of the fit. The second error is from the choice of the resonance model and the parameters (α , T_{cond} , T_{FO} and $\langle u_T \rangle$) of the simulation. The third error is the systematics resulting from slightly different PHENIX and STAR centrality ranges, particle identification and acceptance cuts. These effects have been estimated with Monte-Carlo simulations, detailed in ref.¹⁸, not to exceed 9.8%, 7% and 3% respectively. The main source of systematic errors is the choice of the resonance models. This is due to the unknown initial η' multiplicity, hence models like ref.²⁶ with larger initial η' abundances require smaller in-medium η' mass modification, as compared to the models of ref.^{28,27}.

3.3. Transverse mass spectrum of η' mesons

In addition to the characterization of the in-medium η' mass modification, the transverse momentum spectra of the η and η' mesons have also been reported in Ref.¹⁶. Fig. 4 indicates the reconstructed spectrum of η' mesons in $\sqrt{s_{NN}} = 200$ GeV Au+Au collisions, for simulations based on resonance abundances of Refs.^{27,26}. Normalization was carried out with respect to

the η' multiplicity of the model described in Ref. ²⁶. The spectrum of Fig. 4 features a characteristic low transverse momentum enhancement. Although PHENIX measured before the η spectrum in the $p_T \geq 2$ GeV region ³⁰, as far as we know the spectrum of the η' particles has not been determined before in $\sqrt{s_{NN}} = 200$ GeV Au+Au collisions at RHIC.

The restoration of the $U_A(1)$ symmetry and the symmetry between mass of the η and the η' mesons is illustrated on Fig. 5.

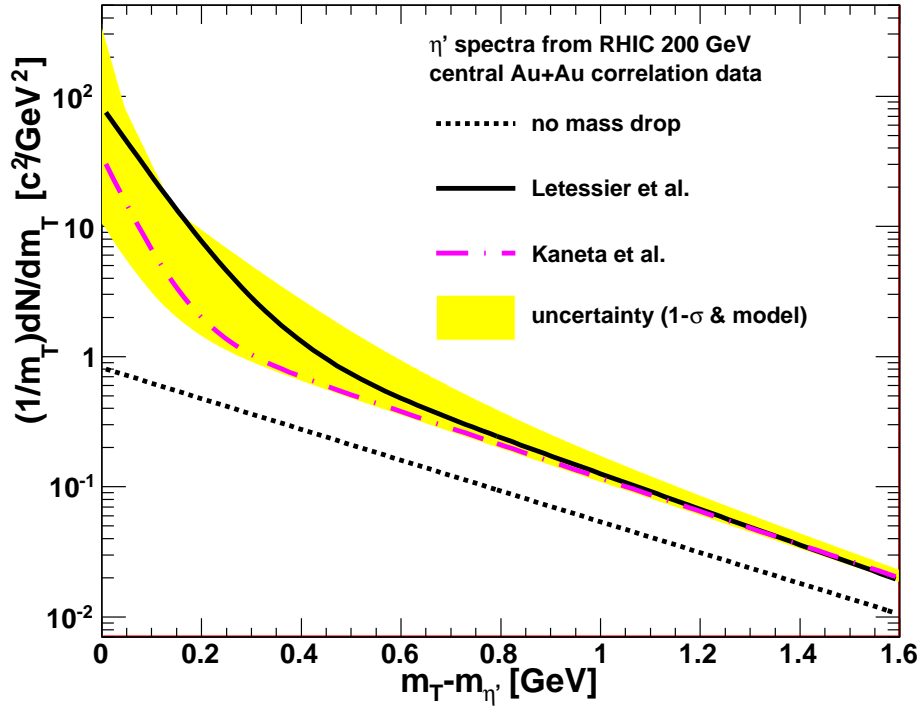


Figure 4. The transverse mass dependent spectrum of the η' mesons, obtained using two different resonance models as input. The band indicates the systematic error, obtained from varying the resonance models as discussed in the text.

4. Discussion

Detailed analysis of the STAR and PHENIX $\lambda_*(m_T)/\lambda_*^{max}$ dataset recorded at 7.7, 9.2, 11.5, 39 and 62.4 GeV during 2010 has just been started ³¹, marking the beginning of the RHIC energy scan program.

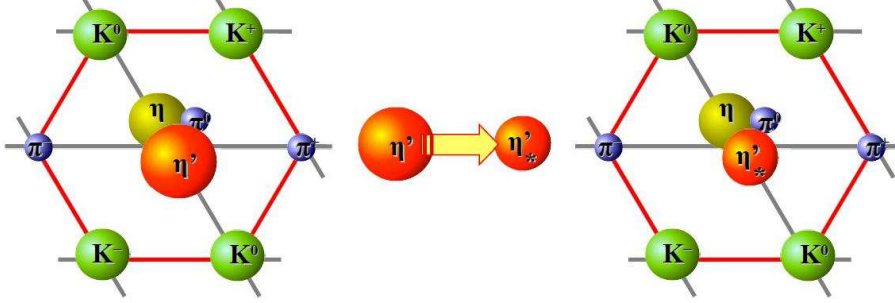


Figure 5. The left hand side plot indicates the 9 pseudoscalar mesons, the size of the pebbles is proportional to the mass, respectively. The central plot indicates that the η' meson reduces its mass in a hot and dense hadronic medium created in Au+Au collisions at RHIC. The right-hand side plot indicates that after the $U_A(1)$ symmetry is effectively restored, the mass of the η and the η' mesons will be similar.

Table 1. Best fits of $m_{\eta'}^*$ and B^{-1} for different resonance multiplicity models, followed by χ^2/NDF and the corresponding confidence level (CL). The integrated η' and η enhancement factors $f_{\eta'}$ and f_{η} are followed by the 5- σ limits of maximum in-medium masses. Errors on $m_{\eta'}^*$ values represent 1- σ boundaries, while the 5- σ limits include systematic errors too.

Resonance model	$m_{\eta'}^*$ (MeV)	B^{-1} (MeV)	$\frac{\chi^2}{NDF}$ (CL %)	$f_{\eta'}$	f_{η}	5- σ limit $m_{\eta'}^*$ (MeV)
ALCOR ²⁵	490^{+60}_{-50}	42	20.2/11 (4.29)	43.4	5.25	≤ 700
Kaneta ²⁶	530^{+50}_{-50}	55	22.8/11 (4.12)	25.6	3.48	≤ 730
Letessier ²⁷	340^{+50}_{-60}	86	18.9/11 (6.35)	67.6	4.75	≤ 570
Stachel ²⁸	340^{+50}_{-60}	86	18.9/11 (6.38)	67.6	4.97	≤ 570
UrQMD ²³	400^{+50}_{-40}	86	18.9/11 (6.14)	45.0	7.49	≤ 660

At present, detailed data are available from the NA44 collaboration at $\sqrt{s_{NN}} = 19.4$ GeV¹³ as well as from the STAR collaboration at $\sqrt{s_{NN}} = 62.4$ and 200 GeV Cu+Cu and Au+Au collisions, the latter at different centrality classes within the 0%–80% range¹². The NA44 data at $\sqrt{s_{NN}} = 19.4$ GeV does not feature an η' mass drop effect. A positive sign of the η' mass modification is apparent in each case of the STAR datasets, indicating that the mass modification effect is nearly at maximum in $\sqrt{s_{NN}} = 200$ GeV Au+Au collisions and reduces with decreasing centrality, colliding energy and system size. We have estimated the magnitude of the system size and energy dependence between 62.4 GeV Cu+Cu and 200 GeV Au+Au collisions to be not larger than 15%, which is substantially less than the

dominant systematic error coming from the choice of the resonance model.

The *dilepton spectrum* has been measured recently in minimum bias Au+Au collisions at $\sqrt{s_{NN}} = 200$ GeV, and a large enhancement was observed in the low invariant mass region $m_{ee} < 1$ GeV³². Low transverse mass enhancement of the η' and η production results in dilepton enhancement just in this kinematic range⁷. Estimations using the enhancement factors in Table 1 indicate that the observed in-medium η' mass drop is indeed a promising candidate to explain this dilepton excess.

PHENIX recently reported a two-component transverse momentum spectrum in dilepton channel *direct photon measurements*³², which provides an additional testing possibility to constrain the two component structure of the η' spectra reported here.

5. Summary

Our report presents a statistically significant, indirect observation of an in-medium mass modification of the η' mesons in $\sqrt{s_{NN}} = 200$ GeV Au+Au collisions at RHIC. These results were recently published in Refs.^{16,17,18}. A similar search for in-medium η' mass modification provided negative result in S+Pb reactions at CERN SPS energies¹⁴. More detailed studies of the excitation function, the centrality and system size dependence of the $\lambda_*(m_T)/\lambda_*^{max}$ could provide important additional information about the onset and saturation of the partial $U_A(1)$ symmetry restoration in hot and dense hadronic matter. Studies of the low-mass dilepton spectrum and measurements of other decay channels of the η' meson may shed more light on the reported magnitude of the low p_T η' enhancement and the related $U_A(1)$ symmetry restoration in high energy heavy ion collisions.

Acknowledgments

We thank the Organizers of the Gribov 80 Memorial Workshop for creating an inspiring scientific atmosphere and providing an excellent setting for scientific discussions. We also would like to thank to professors R. J. Glauber and Gy. Wolf for inspiring and clarifying discussions. T. Cs. is grateful to R. J. Glauber for his kind hospitality at the Harvard University. Our research was supported by Hungarian OTKA grant NK 73143. T. Cs. has also been supported by a Senior Leader and Scholar Fellowship by the Hungarian American Enterprise Scholarship Fund (HAESF).

References

1. A. Adare *et al.* [PHENIX Collaboration], Phys. Rev. Lett. **104**, 132301 (2010) [arXiv:0804.4168 [nucl-ex]].
2. R. Hagedorn, Nuovo Cim. Suppl. **3**, 147 (1965).
3. K. Adcox *et al.* [PHENIX Collaboration], Nucl. Phys. A **757**, 184 (2005) [arXiv:nucl-ex/0410003].
4. A. Adare *et al.* [PHENIX Collaboration], Phys. Rev. Lett. **98**, 162301 (2007) [arXiv:nucl-ex/0608033].
5. E. Shuryak, Nucl. Phys. A **774**, 387 (2006) [arXiv:hep-ph/0510123].
6. T. Kunihiro, Phys. Lett. B **219**, 363 (1989); *ibid.* **245** 687(E) (1990).
7. J. I. Kapusta, D. Kharzeev and L. D. McLerran, Phys. Rev. D **53**, 5028 (1996).
8. Z. Huang and X. N. Wang, Phys. Rev. D **53**, 5034 (1996).
9. Z. Fodor and S. D. Katz, arXiv:0908.3341 [hep-ph].
10. S. S. Adler *et al.*, Phys. Rev. Lett. **93**, 152302 (2004).
11. J. Adams *et al.*, Phys. Rev. C **71**, 044906 (2005).
12. B. I. Abelev *et al.*, Phys. Rev. C **80**, 024905 (2009).
13. H. Beker *et al.*, Phys. Rev. Lett. **74**, 3340 (1995).
14. S. E. Vance, T. Csörgő and D. Kharzeev, Phys. Rev. Lett. **81**, 2205 (1998).
15. T. Csörgő, Heavy Ion Phys. **15**, 1 (2002) [arXiv:hep-ph/0001233].
16. T. Csörgő, R. Vértési and J. Sziklai, Phys. Rev. Lett. **105**, 182301 (2010) [arXiv:0912.5526 [nucl-ex]].
17. R. Vértési, T. Csörgő and J. Sziklai, Nucl. Phys. A **830**, 631C (2009).
18. R. Vértési, T. Csörgő and J. Sziklai, arXiv:0912.0258 [nucl-ex].
19. T. Csörgő and B. Lörstad, Phys. Rev. C **54**, 1390 (1996).
20. S. S. Adler *et al.*, Phys. Rev. C **69**, 034909 (2004).
21. M. Csanád for PHENIX Collaboration, Nucl. Phys. A **774** 611-614 (2006).
22. B. Anderson *et al.*, Nucl. Phys. B **281**, 289 (1987).
23. M. Bleicher *et al.*, J. Phys. G **25**, 1859 (1999).
24. T. Sjöstrand, Comp. Phys. Commun. **82**, 74 (1994).
25. T. S. Biró, P. Lévai and J. Zimányi, Phys. Lett. B **347**, 6 (1995).
26. M. Kaneta and N. Xu, arXiv:nucl-th/0405068.
27. J. Letessier, J. Rafelski, Eur. Phys. J. A **35**, 221 (2008).
28. S. A. Bass *et al.*, Nucl. Phys. A **661**, 205 (1999).
29. S. Weinberg, Phys. Rev. D **11**, 3583 (1975).
30. S. S. Adler *et al.*, Phys. Rev. C **75**, 024909 (2007).
31. B. I. Abelev *et al.*, Phys. Rev. C **81**, 024911 (2010).
32. A. Adare *et al.*, Phys. Rev. C **81**, 034911 (2010).